

Document made available under the Patent Cooperation Treaty (PCT)

International application number: PCT/US05/002556

International filing date: 28 January 2005 (28.01.2005)

Document type: Certified copy of priority document

Document details: Country/Office: US
Number: 60/539,773
Filing date: 28 January 2004 (28.01.2004)

Date of receipt at the International Bureau: 31 March 2005 (31.03.2005)

Remark: Priority document submitted or transmitted to the International Bureau in compliance with Rule 17.1(a) or (b)



World Intellectual Property Organization (WIPO) - Geneva, Switzerland
Organisation Mondiale de la Propriété Intellectuelle (OMPI) - Genève, Suisse

1297601

THE UNITED STATES OF AMERICA

TO ALL TO WHOM THESE PRESENTS SHALL COME:

UNITED STATES DEPARTMENT OF COMMERCE

United States Patent and Trademark Office

March 17, 2005

THIS IS TO CERTIFY THAT ANNEXED HERETO IS A TRUE COPY FROM THE RECORDS OF THE UNITED STATES PATENT AND TRADEMARK OFFICE OF THOSE PAPERS OF THE BELOW IDENTIFIED PATENT APPLICATION THAT MET THE REQUIREMENTS TO BE GRANTED A FILING DATE.

APPLICATION NUMBER: 60/539,773

FILING DATE: *January 28, 2004*

RELATED PCT APPLICATION NUMBER: *PCT/US05/02556*



Certified by

Under Secretary of Commerce
for Intellectual Property
and Director of the United States
Patent and Trademark Office

Under the Paperwork Reduction Act of 1995, no persons are required to respond to a collection of information unless it displays a valid OMB control number.

PROVISIONAL APPLICATION FOR PATENT COVER SHEET

This is a request for filing a PROVISIONAL APPLICATION FOR PATENT under 37 CFR 1.53(c).

Express Mail Label No. EPO21168652US

3441 U.S. PTO
60/539773

012804

INVENTOR(S)					
Given Name (first and middle (if any))	Family Name or Surname	Residence (City and either State or Foreign Country)			
<u>JUSTIN</u>	<u>HANES</u>	<u>Baltimore, MD</u>			
Additional inventors are being named on the <u>one</u> separately numbered sheets attached hereto					
TITLE OF THE INVENTION (500 characters max)					
<u>Drug and Gene Carrier Particles that Rapidly Move Through</u>					
Direct all correspondence to: CORRESPONDENCE ADDRESS					
<input type="checkbox"/> Customer Number: 					
OR					
<input type="checkbox"/> Firm or Individual Name: <u>Johns Hopkins University</u>					
Address: <u>100 N. Charles Street</u>					
Address: <u>5th Floor</u>					
City: <u>Baltimore</u>		State: <u>MD</u>		Zip: <u>21201</u>	
Country: <u>USA</u>		Telephone: <u>410-516-8300</u>		Fax: <u>410-516-5113</u>	
ENCLOSED APPLICATION PARTS (check all that apply)					
<input checked="" type="checkbox"/> Specification Number of Pages <u>30</u>					
<input type="checkbox"/> Drawing(s) Number of Sheets _____					
<input type="checkbox"/> Application Data Sheet. See 37 CFR 1.76					
<input type="checkbox"/> CD(s), Number _____					
<input type="checkbox"/> Other (specify) _____					
METHOD OF PAYMENT OF FILING FEES FOR THIS PROVISIONAL APPLICATION FOR PATENT					
<input checked="" type="checkbox"/> Applicant claims small entity status. See 37 CFR 1.27.					
<input type="checkbox"/> A check or money order is enclosed to cover the filing fees.					
<input type="checkbox"/> The Director is hereby authorized to charge filing fees or credit any overpayment to Deposit Account Number: _____					
<input checked="" type="checkbox"/> Payment by credit card. Form PTO-2038 is attached.					
FILING FEE Amount (\$) \$80.00					
The invention was made by an agency of the United States Government or under a contract with an agency of the United States Government.					
<input type="checkbox"/> No.					
<input checked="" type="checkbox"/> Yes, the name of the U.S. Government agency and the Government contract number are: <u>NSF: CTS0210718</u>					

[Page 1 of 2]

Respectfully submitted,

SIGNATURE [Signature]

TYPED or PRINTED NAME _____

TELEPHONE 410-516-8300

Date 28-JAN-04

REGISTRATION NO. 45,282

(if appropriate)

Docket Number: 4398

USE ONLY FOR FILING A PROVISIONAL APPLICATION FOR PATENT

This collection of information is required by 37 CFR 1.51. The information is required to obtain or retain a benefit by the public which is to file (and by the USPTO to process) an application. Confidentiality is governed by 35 U.S.C. 122 and 37 CFR 1.14. This collection is estimated to take 8 hours to complete, including gathering, preparing, and submitting the completed application form to the USPTO. Time will vary depending upon the individual case. Any comments on the amount of time you require to complete this form and/or suggestions for reducing this burden, should be sent to the Chief Information Officer, U.S. Patent and Trademark Office, U.S. Department of Commerce, P.O. Box 1450, Alexandria, VA 22313-1450. DO NOT SEND FEES OR COMPLETED FORMS TO THIS ADDRESS. SEND TO: Mail Stop Provisional Application, Commissioner for Patents, P.O. Box 1450, Alexandria, VA 22313-1450.

If you need assistance in completing the form, call 1-800-PTO-9199 and select option 2.

PROVISIONAL APPLICATION COVER SHEET
Additional Page

PTO/SB/16 (08-03)

Approved for use through 07/31/2006. OMB 0651-0032

U.S. Patent and Trademark Office; U.S. DEPARTMENT OF COMMERCE

Under the Paperwork Reduction Act of 1995, no persons are required to respond to a collection of information unless it displays a valid OMB control number.

Docket Number 4398

INVENTOR(S)/APPLICANT(S)		
Given Name (first and middle [if any])	Family or Surname	Residence (City and either State or Foreign Country)
Michelle Rose	Dawson	Perry Hall, MD
Eric Mark	Krauland	Somerville, MA
Denis	Wirtz	Washington, DC

[Page 2 of 2]

Number 2 of 2

WARNING: Information on this form may become public. Credit card information should not be included on this form. Provide credit card information and authorization on PTO-2038.

CERTIFICATE OF EXPRESS MAILING

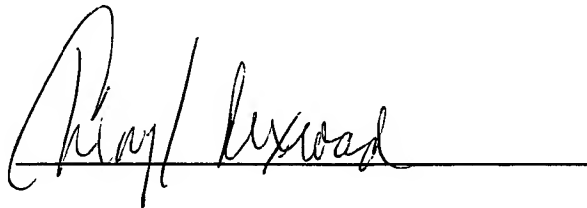
EXPRESS MAILING LABEL NO.

ER021168562US)

I hereby certify that this correspondence (along with any papers referred to as being attached or enclosed) is being deposited with the United States Postal Service as Express Mail, Post Office to Addressee with sufficient postage in a **Flat Rate** envelope addressed to MS Provisional Patent Application, Commissioner for Patents, P.O. Box 1450, Alexandria, VA 22313-1450 on the date indicated below:

28-JAN-04

DATE of Signature
And of Mail Deposit



Signature

This Page Is Inserted by IFW Operations
and is not a part of the Official Record

BEST AVAILABLE IMAGES

Defective images within this document are accurate representations of the original documents submitted by the applicant.

Defects in the images may include (but are not limited to):

- BLACK BORDERS
- TEXT CUT OFF AT TOP, BOTTOM OR SIDES
- FADED TEXT
- ILLEGIBLE TEXT
- SKEWED/SLANTED IMAGES
- COLORED PHOTOS
- BLACK OR VERY BLACK AND WHITE DARK PHOTOS
- GRAY SCALE DOCUMENTS

IMAGES ARE BEST AVAILABLE COPY.

**As rescanning documents *will not* correct images,
please do not report the images to the
Image Problem Mailbox.**

INVENTION INFORMATION

Title of Invention: Drug and gene carrier particles that rapidly move through mucus barriers

Lead Inventor Information: [The Lead Inventor is the primary contact person for LTD on all matters associated with this Report of Invention, including processing, patent prosecution and licensing. For reasons of administrative efficiency, it is the responsibility of the Lead Inventor to keep all other JHU inventors named on this Report of Invention informed of the status of such matters.]

Name of Lead Inventor:

Last: Hanes

First : Justin

Degree: Ph.D.

Title or Position: Assistant Professor

E-mail: hanes@jhu.edu

School: Johns Hopkins University

Department: Chemical and Biomolecular Eng.

Business phone: (410) 516-3484

Business fax: (410) 516-5510

Business address:

Johns Hopkins University, Dept. of Chemical and Biomolecular Engineering, 3400 N. Charles St., Baltimore, MD, 21218.

Interdepartmental address: 221 MD Hall

Home phone number:

Home fax number:

Home address:

5416 Purlington Way
Baltimore, MD 21212

Citizenship: United States

Social Security Number:

Are you an Howard Hughes Medical Institute employee or investigator? ☐ Yes ☒ No

Are you a Kennedy Krieger Institute employee or investigator? ☐ Yes ☒ No

Additional inventors: ☒ Yes ☐ No If yes, please complete Additional Inventors section for each inventor.

LTD Internal Use Only: REF- 4399

TLA CGG

Field of Use _____

ADDITIONAL INVENTOR(S)

Please copy this page for additional inventors as necessary

Name of Inventor:

Last: Dawson

First: Michelle

Middle: Rose

Degree: B.S.

Title or Position: Research Assistant

E-mail: mdawson@jhu.edu

School: Johns Hopkins University

Department: Chemical and Biomolecular Eng.

Business phone: (410) 516-5283

Business fax: (410) 516-5510

Business address:

Johns Hopkins University, Dept. of Chemical and Biomolecular Engineering, 3400 N. Charles St., Baltimore, MD, 21218.

Interdepartmental address:

Home phone number:

Home fax number:

Home address: 1 Capland Ct., Perry Hall, MD 21128.

Citizenship: United States

Social Security Number:

Are you an Howard Hughes Medical Institute employee or investigator?

☐ Yes ☒ No

Are you a Kennedy Krieger Institute employee or investigator?

☐ Yes ☒ No**Name of Inventor:**

Last: Krauland

First: Eric

Middle: Mark

Degree: M.S.

Title or Position: Research Assistant

E-mail: Eric_k@mit.edu

School: MIT

Department: Biological Engineering

Business phone: 617-324-3400

Business fax: 617-324-3300

Business address: MIT, Biological Engineering Department, Bldg. 16-244, 77 Massachusetts Ave., Cambridge, MA 02139.

Interdepartmental address:

Home phone number:

Home fax number:

Home address:

15 Lovell St. Apt 2, Somerville, MA 02144

Citizenship: United States

Social Security Number:

Are you an Howard Hughes Medical Institute employee or investigator?

☐ Yes ☒ No

Are you a Kennedy Krieger Institute employee or investigator?

☐ Yes ☒ No

Name of Inventor:			
Last: Wirtz		First: Denis	Middle: Degree: Ph.D.
Title or Position:	Associate Professor	E-mail: wirtz@jhu.edu	
School: Johns Hopkins University		Department: Chemical and Biomolecular Eng.	
Business phone: (410) 516-7006		Business fax: (410) 516-5510	
Business address: Johns Hopkins University, Dept. of Chemical and Biomolecular Engineering, 3400 N. Charles St., Baltimore, MD, 21218.			
Interdepartmental address: 220 MD Hall			
Home phone number:		Home fax number:	
Home address: 3818 Garrison Street NW, Washington, DC 20016			
Citizenship: Belgian		Social Security Number:	
Are you an Howard Hughes Medical Institute employee or investigator?		<input type="checkbox"/> Yes	<input checked="" type="checkbox"/> No
Are you a Kennedy Krieger Institute employee or investigator?		<input type="checkbox"/> Yes	<input checked="" type="checkbox"/> No

INVENTION DESCRIPTION

Describe the invention completely, using the outline given below. Please provide an **electronic copy** of the invention disclosure document, references, and abstracts in Windows format on CD-ROM or floppy disk if possible

Brief Description of the Invention:

Mucus barriers cover all routes of entry into the body, including the gastrointestinal tract, nose, lungs, and the female reproductive tract. It is critical in many applications that drug delivery particles be able to cross mucus barriers efficiently to ensure the effective delivery of their therapeutic payload to underlying cells.

We formulated sub-200 nm polymer particles using poly (D,L-lactic-co-glycolic) acid (PLGA). These particles can contain entrapped drugs or genes that can be slowly released in the body for prolonged therapies. Drugs or genes can also be attached to the surface of the carriers and slowly released by desorption in the body. For example, we encapsulated a cationic surfactant (DDAB) into the particles and, subsequently, condensed anionic DNA to the surface to obtain gene carriers with 50-fold higher cell transfection rates than naked DNA *in vitro*. Using the method of multiple particle tracking (MPT), we measured the transport rates of dozens of individual PLGA-DDAB/DNA nanoparticles in real time in reconstituted pig gastric mucus (PGM) that possessed physiologically relevant rheological properties. The average transport rate of PLGA-DDAB/DNA nanoparticles was 10-fold higher than similar size polystyrene nanoparticles. Therefore, by changing the surface chemistry of nanoparticles (from hydrophobic like polystyrene to hydrophilic like our PLGA-DDAB/DNA particles), particles that cross mucus barriers much more readily can be produced.

SOFTWARE – Does this disclosure include a software element or software is implemented in the invention?

☐ Yes ☒ No

If yes, please complete the Software Information Sheet which can be found at: _____

BIOLOGICAL MATERIAL – Does this disclosure include biological material?

☒ Yes ☐ No

If yes, please attach a list of materials for reference. A Tangible Property Report of Invention form may be completed if the disclosure is biological materials only. You can find this form at: <http://www.hopkinsmedicine.org/lbd/otl/>

2. Problem Solved:

Drug and gene carrying nanoparticles delivered to mucus-covered epithelial cells in the lung, nose, gastrointestinal and reproductive tracts must traverse mucus to reach cellular targets. Inefficient particle delivery to these tissues has been attributed to slow transport and/or instability of nanoparticles in mucus. Particles, such as those disclosed herein, that remain stable in mucus and move rapidly through this barrier can be used to deliver therapeutic drugs, genes and vaccines, and may be useful in imaging applications in mucosal tissues.

3. Novelty [Identify those elements of the invention that are new when compared to the current state of the art]

- (A) Idea that surface chemistry and particle size can be easily altered to produce particles that more readily cross mucus barriers.
- (B) Fact that DNA coating may render the surfaces of particles less adhesive to mucus.
- (C) DNA coating may be achieved with CpG-rich DNA fragments that are known to be strong immunological adjuvants. This could find use in vaccine applications.
- (D) The particles produced are sub-200 nm in size, which enables them to enter cells once they have traversed the mucus barrier. Entering cells may shelter them from rapid removal mechanisms, thereby enabling them to reside at their target location and deliver drugs over longer periods of time (while wasting less drug).

4. Potential Commercial Use –

- (A) All forms of mucosal drug delivery.
- (B) Mucosal vaccines (including subunit and DNA vaccines).
- (C) Delivery of gene therapeutics to mucus- covered tissues. For example, delivery of CFTR gene to the lungs of patients with cystic fibrosis.

5. Commercialization - List any companies that you feel may be interested in this technology or are doing similar research. Indicate how the invention complements the company's existing technology. If known, provide the names of any companies (and a contact person) who have contacted you regarding your research related to the invention.

Major pharmaceutical companies like Pfizer, Merck, J&J, Genentech, Amgen

Drug delivery companies like Alza, Alkermes

Vaccine delivery companies like Chiron, Corixa

Oral drug delivery companies like Capsugel, Eurand

Pulmonary delivery companies like Nektar, Advanced Inhalation Research, 3M Pharmaceuticals

Gene delivery companies like Valentis, Vical, Copernicus

☐ No company interest known at this time.

Keywords – Please circle the categories and keywords that accurately describe the present invention.

<p>CHEMICAL</p> <ul style="list-style-type: none"> <input checked="" type="checkbox"/> Additives <input type="checkbox"/> Alternative Energy <input type="checkbox"/> Antioxidants <input type="checkbox"/> Batteries <input type="checkbox"/> Catalyst <input type="checkbox"/> Coal Conversion <input checked="" type="checkbox"/> <u>Coatings</u> <input type="checkbox"/> Effluent Treatment <input type="checkbox"/> Elastomers <input type="checkbox"/> Electrochemistry <input type="checkbox"/> Exhaust Treatment <input type="checkbox"/> Foams <input type="checkbox"/> Food Chemistry <input type="checkbox"/> Fuel Cells <input type="checkbox"/> Gas Conversion <input type="checkbox"/> Gels <input type="checkbox"/> Monomers <input type="checkbox"/> Oxidation <input type="checkbox"/> Petroleum <input type="checkbox"/> Photochemistry <input checked="" type="checkbox"/> <u>Polymers</u> <input type="checkbox"/> Remediation <input type="checkbox"/> Solvents <p>DIAGNOSTIC</p> <ul style="list-style-type: none"> <input type="checkbox"/> Antibody <input type="checkbox"/> Assay <input type="checkbox"/> Biochip <input checked="" type="checkbox"/> Contrast Agent (Possible) <input checked="" type="checkbox"/> Detection <input type="checkbox"/> DNA Probe <input type="checkbox"/> Elisa <input checked="" type="checkbox"/> Imaging <input type="checkbox"/> Immunoassay <input type="checkbox"/> In Situ <input type="checkbox"/> Marker <input type="checkbox"/> Measurement <input type="checkbox"/> MRI <input type="checkbox"/> Point of Use <input type="checkbox"/> Radioisotope <input type="checkbox"/> Transgenic <input type="checkbox"/> Ultrasound 	<p>GENOMICS</p> <ul style="list-style-type: none"> <input type="checkbox"/> Allele <input type="checkbox"/> Bioinformatic <input type="checkbox"/> cDNA <input type="checkbox"/> Epidemiology <input type="checkbox"/> EST <input type="checkbox"/> Gene <input type="checkbox"/> Homologue <input type="checkbox"/> Isogene <input type="checkbox"/> Library <input type="checkbox"/> Mutation <input type="checkbox"/> Pharmacogenomics <input type="checkbox"/> Polymorphism <input type="checkbox"/> Positional Cloning <input type="checkbox"/> Proteomics <input type="checkbox"/> Receptor <input type="checkbox"/> RNA <input type="checkbox"/> Target Validation <p>MEDICAL DEVICE</p> <ul style="list-style-type: none"> <input checked="" type="checkbox"/> <u>Delivery</u> <input type="checkbox"/> Diagnosis <input checked="" type="checkbox"/> Imaging <input type="checkbox"/> Measurement <input type="checkbox"/> Optical <input type="checkbox"/> Safety <input type="checkbox"/> Surgical <input checked="" type="checkbox"/> Treatment <p>RESEARCH TOOL</p> <ul style="list-style-type: none"> <input type="checkbox"/> Animal Model <input type="checkbox"/> Antibody <input type="checkbox"/> Cell Line <input type="checkbox"/> Culture <input type="checkbox"/> Directed Evolution <input type="checkbox"/> DNA Probe <input type="checkbox"/> DNA/RNA Sequencing <input type="checkbox"/> DNA/RNA Synthesis <input type="checkbox"/> Electrophoresis <input type="checkbox"/> Elisa <input type="checkbox"/> Enzyme <input type="checkbox"/> Equipment <input type="checkbox"/> Expression System 	<ul style="list-style-type: none"> <input type="checkbox"/> Immunoassay <input type="checkbox"/> Label <input type="checkbox"/> PCR <input type="checkbox"/> Protein Sequencing <input type="checkbox"/> Protein Synthesis <input type="checkbox"/> Reagent <input type="checkbox"/> Spectroscopy <input type="checkbox"/> Tissue Culture <input type="checkbox"/> Vector <p>SCREENING</p> <ul style="list-style-type: none"> <input type="checkbox"/> Assay <input type="checkbox"/> Biochip <input type="checkbox"/> Combinatorial Biology <input type="checkbox"/> Combinatorial Chemistry <input type="checkbox"/> Detection <input type="checkbox"/> HTS <input type="checkbox"/> Phage Display <input type="checkbox"/> Screen <input type="checkbox"/> Target <p>THERAPEUTIC</p> <ul style="list-style-type: none"> <input type="checkbox"/> Analgesic <input type="checkbox"/> Anesthetic <input checked="" type="checkbox"/> Angiogenesis <input checked="" type="checkbox"/> Antibiotic <input checked="" type="checkbox"/> Antibody <input checked="" type="checkbox"/> Antifungal <input checked="" type="checkbox"/> Antiinflammatory <input checked="" type="checkbox"/> Antisense <input checked="" type="checkbox"/> Antiviral <input type="checkbox"/> Apoptosis <input type="checkbox"/> Cell Signaling <input checked="" type="checkbox"/> Cell Therapy <input type="checkbox"/> Disease Model <input checked="" type="checkbox"/> <u>Drug Delivery</u> <input type="checkbox"/> Drug Design <input checked="" type="checkbox"/> Fertility <input checked="" type="checkbox"/> <u>Gene Therapy</u> <input checked="" type="checkbox"/> Hormone <input checked="" type="checkbox"/> <u>Immunotherapy</u> <input type="checkbox"/> Natural Product <input checked="" type="checkbox"/> Peptides 	<ul style="list-style-type: none"> <input checked="" type="checkbox"/> Pro-drug <input checked="" type="checkbox"/> Proteins <input checked="" type="checkbox"/> Small Molecule <input type="checkbox"/> Tissue Engineering <input type="checkbox"/> Transplant <input checked="" type="checkbox"/> Vaccine <input type="checkbox"/> Virus <input type="checkbox"/> Wound Healing <p>DISEASES</p> <ul style="list-style-type: none"> <input type="checkbox"/> Aging <input type="checkbox"/> Blood <input checked="" type="checkbox"/> Cancer <input type="checkbox"/> Cardiovascular <input type="checkbox"/> Dermatologic <input type="checkbox"/> Endocrine <input checked="" type="checkbox"/> Gastrointestinal <input checked="" type="checkbox"/> Genitourinary <input type="checkbox"/> Hepatic <input checked="" type="checkbox"/> Immune <input checked="" type="checkbox"/> Infectious <input type="checkbox"/> Metabolic <input type="checkbox"/> Musculoskeletal <input type="checkbox"/> Neurological <input checked="" type="checkbox"/> ObGyn <input checked="" type="checkbox"/> Ophthalmological <input checked="" type="checkbox"/> Oral <input checked="" type="checkbox"/> Pediatric <input type="checkbox"/> Psychiatric <input checked="" type="checkbox"/> Respiratory <p>ADDITIONAL KEY WORDS:</p> <p>_____</p> <p>_____</p> <p>_____</p> <p>STAGE OF DEVELOPMENT</p> <ul style="list-style-type: none"> <input type="checkbox"/> Unspecified <input type="checkbox"/> Discovery <input checked="" type="checkbox"/> Preclinical <input type="checkbox"/> Prototype <input type="checkbox"/> Phase I <input type="checkbox"/> Phase II <input type="checkbox"/> Phase III <input type="checkbox"/> NCE
--	--	---	---

7. Detailed Description of the invention - On a separate page(s), attach a detailed description of how to make and use the invention. The description must contain sufficient detail so that one skilled in the same discipline could reproduce the invention. Include the following as necessary:

- | | |
|--|---|
| 1- data pertaining to the invention; | 4- procedural steps if a process |
| 2- drawings or photographs illustrating the invention; | 5- a description of any prototype or working model; |
| 3- structural formulae if a chemical; | |

In general, a manuscript that has been prepared for submission to a journal will satisfy this requirement.

8. Workable Extent/Scope [Describe the future course of related work, and possible variations of the present invention in terms of the broadest scope expected to be operable; if a *compound*, describe substitutions, breadth of substituents, derivatives, salts etc., if *DNA or other biological material*, describe modifications that are expected to be operable, if a *machine or device*, describe operational parameters of the device or a component thereof, including alternative structures for performing the various functions of the machine or device]

- (A) any polymer or water-insoluble material may be used to make the particles
- (B) any chemical capable of altering the surface of the nanoparticles to make them less adhesive to mucus can be adsorbed (including DNA, surfactants, proteins, sugars, peptides, etc.)
- (C) size range of 100 um or less may work, but preferred size may be less than 500 nm

9. References [Please cite relevant journal citations, patents, general knowledge or other public information related to the invention and distinguish between references that (A) contain a description of the current invention from those that (B) contains background information.]

(A) Description of current invention

Dawson M, Krauland E, Wirtz D, Hanes J, Transport of polymeric nanoparticle gene carriers in gastric mucus, *Biotech Prog*, in press (attached).

☐ No references available at this time.

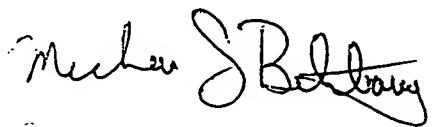
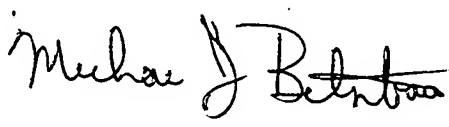
ACKNOWLEDGMENT, CERTIFICATION and ASSIGNMENT OF INVENTION

In order for this Report of Invention to be complete and processed by LTD, it must be signed and dated by:

- (1) the JHU Department Director for each JHU department involved with the development of this invention (SECTION A), and,
- (2) ALL Inventors (SECTIONS B and C), including those Inventors not subject to The Johns Hopkins University Intellectual Property Policy. Each Inventor must complete only one of Sections B or C (See explanations in the following sections).
- (3) Please duplicate Sections A, B and/or C as needed for proper completion with ALL appropriate signatures.

SECTION A. JHU SCHOOL and DEPARTMENT DIRECTOR'S ACKNOWLEDGEMENT

I have read and understood this Report of Invention.

 JHU Department Director Signature	Justin Hanes _____ Typed or Printed Name Chemical & Biomolecular Engineering Whiting School of Engineering _____ JHU Department and School	 Date 1/15/04
 JHU Department Director Signature	Michelle Dawson _____ Typed or Printed Name Chemical & Biomolecular Engineering Whiting School of Engineering _____ JHU Department and School	 Date 1/15/04
 JHU Department Director Signature	Eric Krauland _____ Typed or Printed Name Biomedical Engineering _____ JHU Department and School	 Date


JHU Department Director Signature

Denis Wirtz

Typed or Printed Name

Chemical & Biomolecular Engineering
Whiting School of Engineering

JHU Department and School

Date

1/15/04

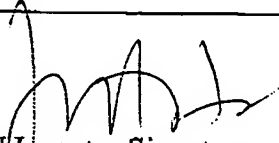

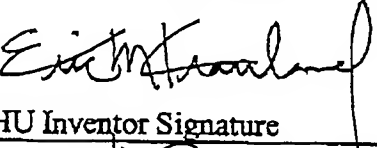

SECTION B. JHU INVENTOR CERTIFICATION and ASSIGNMENT

This section is to be completed only by those JHU personnel subject to The Johns Hopkins University Intellectual Property Policy. Non-JHU Inventors, and HHMI or KKI Inventors at JHU are subject to a separate assignment and must complete Section C. JHU Inventors who believe they are not subject to The Johns Hopkins University Intellectual Property Policy for the invention described herein must complete Section C.

I/we, the Inventors, hereby certify that the information set forth in this Report of Invention is true and complete to the best of my/our knowledge.

I/we, the Inventors, hereby certify that I/we will promptly advise LTD of any commercial interest regarding the invention described herein.

I/we, the Inventor(s), subject to The Johns Hopkins University Intellectual Property Policy and not under an obligation to assign intellectual property rights to another party, hereby affirm that in consideration for The Johns Hopkins University's evaluation of commercial potential and a share of income which I/we may receive upon commercialization of my/our invention, on the date of my/our signature(s) as indicated below do hereby assign and transfer my/our entire right, title and interest in and to the invention described herein unto The Johns Hopkins University, its successors, legal representatives and assigns.

 JHU Inventor Signature	Justin Hanes Typed or Printed Name	1/15/04 Date
		% of Contribution 40
 JHU Inventor Signature	Michelle Dawson Typed or Printed Name	1-15-2004 Date
		% of Contribution 20
 JHU Inventor Signature	Eric Krauland Typed or Printed Name	1-14-2004 Date
		% of Contribution 20
 JHU Inventor Signature	Denis Wirtz Typed or Printed Name	1-15-2004 Date
		% of Contribution 20
The Johns Hopkins University Intellectual Property states that inventorship contribution is equal unless otherwise agreed upon. Inventorship contribution provides for potential revenue and cost sharing. JHU inventor's percentages must TOTAL 100%.		JHU INVENTOR'S TOTAL 100 %

reported catalytic activity in an all-RNA subdomain of the spliceosome containing U2, U6, and a branch oligonucleotide.¹ This result is intriguing in that it suggests that the spliceosome may act as a ribozyme. Previous studies show that the formation of a U2-U6 complex plays a pivotal role in this suggested catalytic activity.² Our goal is to characterize this U2-U6 complex using various structure-probing techniques. Thermal denaturation and non-denaturing gel electrophoresis studies were performed to investigate complex formation. To further probe the folding of U2-U6 and the potential metal sites associated with this complex, hydroxyl radical footprinting and analytical ultracentrifugation experiments will be performed.

¹ Valadkhan, S. & Manley, J.L., *Nature*, 413, 701-707 (2001)

² Valadkhan, S. & Manley, J.L., *RNA*, 6, 206-219 (2000)

3100-Pos Board #B352 DNA Mapping with TIRF Wide-Field Microscopy and Centroid Localization

Xiaohui Qu¹, Laurens Mets², Norbert F. Scherer³

¹Department of Physics, Institute for Biophysical Dynamics, University of Chicago, Chicago, IL, USA, ²Department of Molecular Genetics and Cell Biology, University of Chicago, Chicago, IL, USA, ³Department of Chemistry, Institute for Biophysical Dynamics, University of Chicago, Chicago, IL, USA.

The sequence of DNA provides fundamental information for understanding biological behavior. Conventional restriction mapping can provide useful characterization of small DNA molecules, but throughput is low and it fails for complex DNA. Here we employ a fluorescence mapping strategy; DNA is labeled with single fluorophore bis-PNA probes that recognize short sequence sites (6 or 7 bases). Using TIRF wide field microscope and centroid localization, the position of the dye molecule on each bis-PNA is determined within a few nanometers, dependent upon the total number of photons emitted by the dye. Making use of abrupt photobleaching of single dye photon emission and almost constant emission intensity on a time scale of seconds, multiple dyes within the point spread function are also resolved with a few nanometer precision. Thus, a physical map, showing the relative locations of landmark sequence features along DNA can be obtained with high resolution. This approach to single molecule mapping works for both short and long DNA. We have established the validity of the method and are working on optimizing the experimental conditions for mapping.

3101-Pos Board #B353 Real-Time Tracking of Nanoparticle Gene Carriers in Gastrointestinal Mucus

Michelle Dawson, B.S., Denis Wirtz, Ph.D., Justin Hanes, Ph.D.,
Chemical and Biomolecular Engineering, Johns Hopkins University,
Baltimore, MD, USA.

Nanoparticle transport through mucosal barriers is often restricted owing to mucoadhesive forces and the highly viscoelastic nature of mucus gels, which may limit efficient drug and gene delivery. We formulated sub-200 nm particles from poly (D,L-lactic-co-glycolic) acid (PLGA) and the cationic surfactant, DDAB. Subsequently, anionic DNA was condensed to the surface to obtain non-cytotoxic gene carriers, with *in vitro* transfection efficiencies that were 50-fold higher than naked DNA. Using the method of multiple particle tracking (MPT), we measured the transport rates of dozens of individual PLGA-DDAB/DNA nanoparticles in real time in reconstituted pig gastric mucus (PGM) that possessed physiologically relevant rheological properties. The average transport rate of PLGA-DDAB/DNA nanoparticles was 10-fold higher than similar size polystyrene nanoparticles. Furthermore, PLGA-DDAB/DNA nanoparticles appeared to be more mobile than COOH-PS nanoparticles. The observation that PLGA-DDAB/DNA particles moved faster on average than PS particles was somewhat counterintuitive since PLGA-DDAB/DNA nanoparticles formed large aggregates in pig gastric mucus, which were expected to reduce their transport rates. This result may indicate that particle transport was positively affected by the formation of mucus-particle aggregates that may have increased pore diameters of the surrounding network, promoting more rapid transport of free particles. By measuring individual particle transport rates, we determined that a small but significant percentage of very fast moving particles in mucus were largely responsible for the increase in transport rates of PLGA-DDAB/DNA nanoparticles. Improved transport rates, stability in mucus, and ability to transfect cells make PLGA-DDAB/DNA nanoparticles candidates for mucosal DNA vaccines and gene therapy.

3102-Pos Board #B354

Tracking of dual-labeled SiHybrid gene-silencing Molecules in individual Human Cells using Confocal Laser Scanning Microscopy
Lawrence Dugan, Ph.D., Thomas Huser, Allen Christian
PBI/BBRP, Lawrence Livermore National Laboratory, Livermore, CA, USA.

RNA interference is a highly conserved process by which cells degrade unwanted mRNA in a sequence-specific manner using small, interfering RNA molecules (siRNA). These siRNA molecules can be made synthetically and induce the same effect in cells. We have modified the structure of siRNA from double-stranded RNA to RNA:DNA, termed SiHybrids, and have seen improved gene silencing effects, including longevity and level of effect. Initial fluorescence imaging efforts involving the RNA strand with Cy-3 indicated cytoplasmic uptake of the SiHybrid molecules <24 hours after transfection. With this method we could easily detect large quantities of labeled molecules within the cytoplasm of cells using an inverted epifluorescence microscope. Currently, we are using confocal scanning laser microscopy to track and quantify the presence and amount of dual-labeled SiHybrid molecules in individual human HeLa cells. These SiHybrid molecules were labeled with Cy-3 on the RNA strand and Cy-5 on the DNA strand and cultured in glass bottom dishes. We used dual-labeling to track which of the strands is involved in the gene silencing process. SiHybrid molecules were introduced into the culture media without transfection reagent, where they were then taken up by cells. Preliminary imaging results indicate that the SiHybrid molecules are readily taken up into the cytoplasm. We are currently tracking the presence of very low numbers of dual-labeled SiHybrid molecules as a function of time, cell generation and initial concentration.

This work was performed under the auspices of the U. S. Department of Energy by the University of California, Lawrence Livermore National Laboratory under Contract No. W-7405-Eng-48.

Single Molecule Biophysics III

3103-Pos Board #B355

A novel approach for sensing single-molecule motion using a variable-width capacitor

Ziv Reich¹, Ilan Sagiv², Guy Ziv³, Dan Shahar², Noa Mazorski⁴, Joseph Shappir⁴, Ruti Kapon¹

¹Biological Chemistry, Weizmann Institute of Science, Rehovot, Israel,

²Condensed Matter Physics, Weizmann Institute of Science, Rehovot, Israel,

³Physics of Complex Systems, Weizmann Institute of Science, Rehovot, Israel,

⁴Center for Nano-Science and Nano-Technology, Hebrew University of Jerusalem, Jerusalem, Israel.

We present a novel approach to study the real-time dynamics of single molecules using electrical measurements. The method is based on the use of a *nonparallel-plate* capacitor. A particle moving within such a capacitor induces capacitance changes that depend on its position. Monitoring these changes allows motion to be traced at a resolution better than the smallest fabricated feature of the device. A micron scale triangular sensor based on this concept was fabricated using Si micromachining technology. Using this device we were able to follow the motion of gold and silica microspheres suspended in glycerol at sub-micron resolution. The detection scheme also enables the distinction between particles based on their dielectric constants. In addition, the special geometry of the capacitor, establishes an electric field gradient within, which exerts a dielectrophoretic force on the particles. This force can be controlled with high precision and at short time scales by modulating the voltage on the capacitor plates, allowing for force spectroscopy measurements simultaneously with the motion measurements. This new approach provides a means for studying various aspects of single-particle dynamics at high resolution, in real time, in liquid and under conditions compatible with biological systems.

3104-Pos Board #B356

High-bandwidth microrheology applied to solutions and networks of semiflexible biopolymers

Karim M. Addas, PhD student in Physics¹, Christoph Schmidt, Professor of physics², Jay Tang, Assistant professor of physics³

¹Physics, Indiana University, Bloomington, IN, USA, ²Physics of Complex

Systems, Vrije Universiteit, Amsterdam, Netherlands, ³Physics, Brown

University, Providence, RI, USA.

Semiflexible protein filament networks are characteristic of the cytoskeleton and the extracellular matrix, and their dynamics over a broad range of time and length scales are at the basis of cellular mechanics. We have developed one and two-particle microrheology, employing micron-sized embedded beads and laser trapping combined with interferometric displacement detection, to study the rheological properties of mono-disperse semiflexible fd-virus solutions. We have tested these relatively new techniques

Transport of Polymeric Nanoparticle Gene Carriers in Gastric Mucus

Michelle Dawson,[†] Eric Krauland,[‡] Denis Wirtz,^{†,§} and Justin Hanes^{*,†,‡}

Departments of Chemical and Biomolecular Engineering, Biomedical Engineering, and Materials Science and Engineering, The Johns Hopkins University, Baltimore, Maryland

Nanoparticle transport through mucosal barriers is often restricted owing to mucoadhesion and the highly viscoelastic nature of mucus gels, which may limit efficient drug and gene delivery. We formulated sub-200 nm particulates from poly(D,L-lactic-co-glycolic) acid (PLGA) and the cationic surfactant dimethyldioctadecylammonium bromide (DDAB). Subsequently, anionic DNA was condensed to the surface to obtain gene carriers with transfection rates 50-fold higher than those of naked DNA *in vitro*. Using the method of multiple particle tracking (MPT), we measured the transport rates of dozens of individual PLGA-DDAB/DNA nanoparticles in real time in reconstituted pig gastric mucus (PGM) that possessed physiologically relevant rheological properties. The average transport rate of PLGA-DDAB/DNA nanoparticles was 10-fold higher than those of similar size polystyrene nanoparticles. Improved transport rates, stability in mucus, and ability to transfect cells make PLGA-DDAB/DNA nanoparticles candidates for mucosal DNA vaccines and gene therapy.

Introduction

Cationic polymeric microparticles have previously been shown to efficiently condense DNA, leading to noncytotoxic gene carriers capable of stable gene expression in small animal models following intramuscular injection (1–3). In these studies, the effective dosage of DNA was reduced from 1–2 mg to 1–10 μ g, a result attributed to the reduced degradation of DNA (since encapsulation leads to DNA degradation) and the enhanced amount of DNA immediately available to induce an immune response.

Mucosal immunization is of considerable interest since gastrointestinal, nasal, respiratory, and vaginal mucosal tissues all drain to lymph nodes, leading to both local and distal immune responses (4). Thus, immunization of one mucosal surface can lead to long-term protective immune responses on all other mucosal surfaces. However, the effectiveness of cationic nanoparticles to deliver DNA to mucosal sites relies on the ability of these particles to cross mucosal barriers (5, 6).

The primary component of mucus is high molecular weight mucin glycoproteins, which form numerous covalent and noncovalent bonds with other mucin molecules and various constituents, including DNA, alginate, and hyaluronan (5). Reconstituted mucus formulated from pig gastric, human cervical, and tracheobronchial mucins display similar mucus structures, with large rod or fiberlike aggregates of 5 nm in diameter and 100–5000 nm in length (7). The condensed and complex microstructure of the mucus network gives rise to a highly viscoelastic gel, which significantly impedes the transport rates of large macromolecules and nanoparticles (8–10).

Immobilized nanoparticles are subject to bacterial and enzymatic degradation and may also be cleared from the body by normal mucus clearance mechanisms. Although clearance rates are anatomically determined, mucus turnover rates in the GI tract are estimated as between 24 and 48 h (7). In the lungs, clearance rates are dependent on the region of particle deposition; however, normal tracheal mucus velocities, albeit more rapid than mucus velocities in the peripheral lung, range from 1–10 mm/min and turnover times are less than 1 h (11). As a result, it is imperative that drug and gene carriers designed to deliver their payload to epithelial cells be capable of efficiently traversing mucus layers coating mucosal surfaces.

In this study, cationic polymeric nanoparticles were formulated from a biocompatible and biodegradable polymer (poly(D,L-lactic-co-glycolic) acid, PLGA), cationic surfactant (dimethyldioctadecylammonium bromide, DDAB) and DNA, leading to positively charged particles with average sizes <200 nm in diameter. These particles aggregated slightly upon addition to mucus solutions reconstituted from pig gastric mucin, whereas 200 nm carboxylated polystyrene (COOH-PS) particles did not. Despite this fact, PLGA-DDAB/DNA particles exhibited average transport rates 10-fold higher than those of COOH-PS particles in gastric mucus.

Materials and Methods

Materials. Poly(D,L-lactic-co-glycolic) (PLGA) (Medisorb High I.V. 54:46) was obtained from Alkermes (Cincinnati, OH), and 1,2-diacyl-palmitoyl-glycerol-3-phosphocholine (DPPC) was purchased from Avanti Polar Lipids (Alabaster, AL). Dimethyldioctadecylammonium bromide (DDAB), bovine serum albumin (BSA), pig gastric mucin (PGM), and deoxyribonucleic acid (DNA) (sodium salt, from salmon testes) were purchased from Sigma (St. Louis, MO) and used without further purification. 2,2,2-Trifluoroethanol (TFE) was purchased from

* To whom correspondence should be addressed. Ph: (410) 516-3484. Fax: (410) 516-5510. Email: hanes@jhu.edu.

[†] Chemical and Biomolecular Engineering.

[‡] Biomedical Engineering.

[§] Materials Science and Engineering.

Fluka (Milwaukee, WI). Plasmid DNA was extracted from *Escherichia coli* culture (strain DH5a, plasmid p43-clz1, kindly donated by Dr. Kam Leong, Johns Hopkins University) grown in freshly prepared Luria Bertani (LB) broth supplemented with 100 mg/mL ampicillin (Kodak Chemicals, Rochester, NY) using a Endo-free Qiagen Megaprep (Valencia, CA) and subsequently resuspended in sterile, deionized water. The plasmid p43-clz1 contains the β -galactosidase gene under the human early-intermediate cytomegalovirus (CMV) promoter and also contains a gene for ampicillin resistance. All other solutions and reagents were of analytical grade and used without further purification.

Formulation of Cationic PLGA Nanoparticles.

Particles were prepared by a solvent extraction/precipitation method. PLGA (3 mg/mL) and DDAB (10 mg/mL) were dissolved in TFE separately. Subsequently, 3 mL of PLGA solution (9 mg PLGA) and 200 μ L of DDAB solution (2 mg DDAB) were combined and added dropwise to 8 mL of filtered distilled water stirring on a magnetic plate. Next, 100 μ L of 1 mg/mL salmon testes DNA in distilled water was added to the water/TFE mixture and stirred for 3 h on a magnetic plate to allow for TFE evaporation. The final formulation was 1.1% DNA to PLGA (w/w) and 5% DNA to DDAB (w/w). The nanoparticle suspension was then passed through a 1 μ m Watman syringe filter (Kent, UK) to remove large impurities and subsequently spun down for 75 min at 15,000 $\times g$ and 4 $^{\circ}$ C using a Beckman-Coulter Avanti J-25 centrifuge (Fullerton, CA) to pellet nanoparticles. Spin conditions were carefully chosen as to not spin down cationic lipid/DNA particles. PLGA-DDAB/DNA nanoparticles were resuspended in distilled water and lyophilized or used directly for characterization or transport studies.

Nanoparticle Characterization. The size and surface morphology of the nanoparticles were examined by transmission electron microscopy. Nanoparticles in suspension were adsorbed to carbon-coated ionized Formvar grids, negatively stained with 2% uranyl acetate, and observed with Philips 420 transmission electron microscope (Eindhoven, Netherlands).

The size and ζ -potential of the nanoparticles were determined by dynamic light scattering and laser Doppler anemometry, respectively, using a Zetasizer 3000 (Malvern Instruments, Southborough, MA). Size measurements were performed at 25 $^{\circ}$ C at a scattering angle of 90 $^{\circ}$. Samples were diluted in 150 mM NaCl with or without pig gastric mucin (PGM) (final mucin concentration was 10 mg/mL). ζ -Potential measurements were performed according to instrument instructions with samples diluted in 150 mM NaCl with or without PGM (final mucin concentration was 2 mg/mL).

Gel electrophoresis (Mini-sub cell GT, Bio-rad, Hercules, CA) was used to verify the binding of DNA to particles and the necessity for cationic surfactants in the DNA adsorption process. Twenty microliters of sample was run on an ethidium bromide stained 1.0% agarose gel (70 V for 60 min) in TAE buffer (Tris-Acetate-EDTA).

Nanoparticle and Naked DNA Transfections with Lac-Z Reporter Gene. Cos-7 cells were obtained from American Type Culture Collection (ATCC, Rockville, MD) and maintained in Dulbecco's Modified Eagle's Medium (DMEM) (Gibco, BRL) containing 10% fetal bovine serum (Gibco, BRL, Invitrogen Co., Carlsbad, CA). Cells seeded at a density of 1.8×10^6 cells/cm 2 on 35-mm 6-well plates were transfected at 50–60% confluency with PLGA-DDAB/DNA nanoparticles or plasmid DNA alone (the concentration in all cases was maintained to yield 2.5

μ g DNA per well, or 0.26 μ g DNA/cm 2). Cells were harvested 48 h after transfection. β -Galactosidase activity and total protein content were assayed using the standard β -galactosidase spectrophotometric assay (12) and the manufacturer's given micro-well protocol for the BCA assay (Pierce Chemical Co., Rockford, IL), respectively. Reported values of β -galactosidase expression were normalized to the total protein content per sample well ($n = 3$).

The toxicity of PLGA-DDAB/DNA nanoparticles to Cos-7 cells was assayed using a propidium iodide nucleic acid stain (Molecular Probes, Eugene, OR). Cos-7 cells seeded at 1×10^6 cells/cm 2 were allowed to reach 60% confluency and then incubated with PLGA-DDAB/DNA nanoparticles, naked DNA, or PolyFect/DNA particles and harvested after 48 h. The PLGA-DDAB/DNA particle volume was adjusted to give final DNA amounts of 1.0, 2.5, and 5.0 μ g per well, and naked DNA and PolyFect/DNA concentrations were adjusted to result in a final DNA content of 2.5 μ g per well. Harvested cells were resuspended in 500 μ g/mL propidium iodide solution, which intercalates with DNA released from necrotic cells. The percentage of dead cells was assayed using flow cytometry. Adsorption and emission maxima for propidium iodide are 535 and 617 nm.

Formulation and Characterization of Reconstituted Pig Gastric Mucus (PGM). Mucus was formulated from 60 mg/mL PGM, 3.2 mg/mL DPPC, and 32 mg/mL BSA in sputum buffer (85 mM Na $^+$, 75 mM Cl $^-$, 20 mM Hepes, pH 7.4) (9). Mucus was mixed on a stir plate for 48 h at 4 $^{\circ}$ C and stored at -20° C (9).

Rheological characterization of gastric mucus was performed with a strain controlled cone-and-plate rheometer (ARES-100, Rheometrics, Piscataway, NJ) as previously described (13, 14). Dynamic tests were performed at 25 $^{\circ}$ C, and buffer evaporation was eliminated using a vapor trap. We report the time-dependent in-phase component of the stress divided by the amplitude of applied oscillatory deformation of fixed frequency, $G'(\omega)$, the out-of-phase component, $G''(\omega)$, and the phase angle, $\phi = \tan^{-1}(G''/G')$. G' and G'' are also commonly referred to as the elastic and viscous moduli, respectively.

Confocal images of particles embedded in reconstituted mucus were captured with an AxioCAM HR camera attached to a Zeiss LSM 510 Meta laser scanning confocal microscope. Mucus was placed in a Biopetechs thermal regulated chamber (Biopetechs, Butler, PA) maintained at 37 $^{\circ}$ C. Three-dimensional images were reconstructed using Metamorph software (Universal Imaging Corp., West Chester, PA).

Nanoparticle Transport Rates in PGM with Multiple Particle Tracking (MPT). Trajectories of fluorescently labeled carboxylated polystyrene particles (COOH-PS; Molecular Probes; -5 mV ζ -potential at pH 6; 200 nm diameter) and PLGA-DDAB/DNA nanoparticles with condensed salmon testes DNA (35 mV, 196 ± 29 nm diameter) in reconstituted PGM were recorded using a silicon-intensified target camera (VE-1000, Dage-MTI, Michigan, IN) mounted on an inverted epifluorescence microscope equipped with 100X oil-immersion objective (numerical aperture 1.3). The trajectories of $n = 109$ COOH-PS and $n = 120$ PLGA-DDAB/DNA particles were tracked in PGM samples contained within a microscope chamber maintained at 37 $^{\circ}$ C.

The centroid of each particle was tracked with 5 nm spatial resolution, determined by tracking the apparent displacements of microspheres immobilized on a glass microslide with a strong adhesive (15). Nanoparticle motion was tracked in 2-D by following the motion of

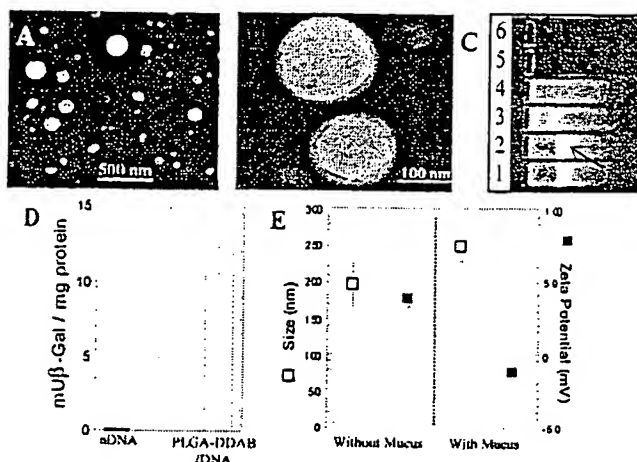


Figure 1. Characterization of PLGA-DDAB/DNA nanoparticles. (A, B) Transmission electron micrographs showed nanoparticle sizes < 300 nm. (C) Complexation of salmon testes DNA with cationic PLGA-DDAB nanoparticles was assayed by UV gel electrophoresis. Lanes 1 and 2: free DNA (arrow shows primary band ~ 2 kb). Lanes 3 and 4: PLGA-DNA (no DDAB). Lanes 5 and 6: PLGA-DDAB/DNA nanoparticles. (D) PLGA-DDAB/DNA nanoparticles transfect Cos-7 cells with 50-fold increase in transfection efficiency compared to naked DNA. (E) The size and ζ -potential of PLGA-DDAB/DNA nanoparticles were assayed in 150 mM NaCl and in PGM. Size values represent the average value from 10 measurements, while the ζ -potential values were an average of three measurements ($n = 2$ separate batches).

nanoparticles in the plane of focus. For 2-D displacements to accurately represent 3-D motion, the fluid must be isotropic but need not be homogeneous (14). Images of the microspheres were captured with a custom routine incorporated in the Metamorph software (Universal Imaging Corp.) at a frequency of 30 Hz for 20 s, which gives a temporal resolution of 33 ms. The coordinates of nanoparticle centroids were transformed into families of time-averaged mean squared displacements (MSD), $\langle \Delta^2(\tau) \rangle = \langle [x(t+\tau) - x(t)]^2 + [y(t+\tau) - y(t)]^2 \rangle$ (τ = time scale or time lag), from which distributions of MSDs and time-dependent particle diffusion coefficients ($D(\tau) = \langle \Delta^2(\tau) \rangle / 4\tau$) were calculated as previously demonstrated (16). Diffusion coefficients were normalized with the theoretical diffusion coefficient of 200 nm particles in water as determined by the classical Stokes-Einstein equation.

Results and Discussion

Cationic microparticles with DNA adsorbed to their surfaces have been shown to efficiently transfect cells in vitro (1-3, 17). However, obtaining high transfection efficiencies in vivo is often limited by particle transport through extracellular barriers, including the mucosal barrier, which has been described as the foremost barrier to transfection in mucus-covered cells (5, 18, 19). To determine if cationic nanoparticles formulated from PLGA and DDAB with condensed DNA may be effective gene carriers for administration to mucosal sites, we produced PLGA-DDAB/DNA nanoparticles and studied their transport rates in reconstituted pig gastric mucus (PGM). Reconstituted PGM was found to have compositional and rheological properties physiologically relevant to gastrointestinal (GI), nasal, and respiratory mucus (7).

PLGA-DDAB/DNA Nanoparticle Characterization. PLGA-DDAB/DNA nanoparticles with sizes less than 200 nm (Figure 1A and B) can be designed to tightly bind DNA with high efficiency (Figure 1C). In addition, their small size compared to previous cationic particles in the micron-range (1-3, 17) allows them to enter cells,

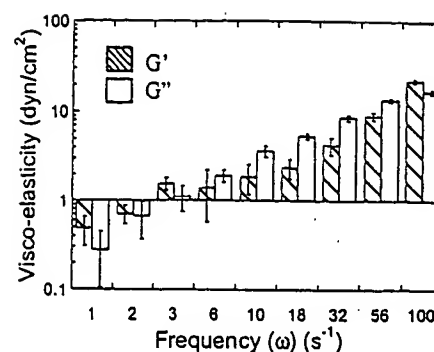


Figure 2. Elastic (G') and viscous (G'') moduli of reconstituted pig gastric mucus ($n = 3$). Note that at low frequencies PGM acts more elastic than viscous, with phase angle, $\phi = \tan^{-1}(G''/G') \sim 30^\circ$, but it yields at low frequency (2.5 s^{-1}) and the phase angle shifts to $\phi \sim 50^\circ$.

either through nonspecific or receptor-mediated endocytosis. Similar to the results that Singh found with cationic microparticles (1, 2), the transfection efficiency of PLGA-DDAB/DNA nanoparticles was 50-fold higher than that of naked DNA (Figure 1D). At the concentration used in the transfection study, PLGA-DDAB/DNA nanoparticles ($16.6 \pm 6.2\%$ dead cells) were less toxic than PolyFect/DNA particles containing the same amount of DNA ($23.9 \pm 1.2\%$ dead cells) but more toxic than naked DNA alone ($4.7 \pm 2.4\%$ dead cells). The toxicity of PLGA-DDAB/DNA nanoparticles showed a dose-dependency with slightly lower particle concentrations (corresponding to $1 \mu\text{g}$ DNA total, or 2.5-fold lower concentration than used in the transfection study) resulting in background levels of cell toxicity ($7.2 \pm 0.6\%$ dead cells, not significantly different than naked DNA controls). Singh and co-workers reported that PLGA-DDAB/DNA microparticles caused no acute toxicity with particle doses resulting in the equivalent of 1 mg of DNA per animal (guinea pig) (1).

Incubation of PLGA-DDAB/DNA nanoparticles in mucus for < 30 min changed the average particle surface charge from $39 \pm 6 \text{ mV}$ to $-11 \pm 7 \text{ mV}$, and the average particle size increased from $196 \pm 29 \text{ nm}$ to $249 \pm 21 \text{ nm}$. The change in size and surface charge of PLGA-DDAB/DNA particles indicated that mucus constituents adsorbed on particle surfaces, leading to a significant increase in particle diameter.

Rheological Characterization of PGM. The highly viscoelastic properties and gel formation of mucus (phase angle $< 45^\circ$) arise primarily from the high molecular weights and expanded conformations of mucin glycoproteins in aqueous solution. The ability of mucus to undergo gelation is also strongly affected by the concentrations of lipids and macromolecules, which noncovalently interact with mucins promoting the formation of larger mucin fibers that overlap to form dense mucus networks (20, 21). Physiologically, the high viscoelasticity of mucus gels is maintained to provide a barrier to microbial and particle transport; high elasticity also allows mucus to be engaged by ciliated cells or moved by pulsatory forces as it is cleared from the body (20). The viscous and elastic properties are properly matched in vivo to achieve appropriate mucus clearance rates (5, 20).

The frequency-dependent elastic and viscous moduli were used to characterize the viscoelastic nature of reconstituted pig gastric mucus (PGM) used in this study (Figure 2). The phase angle of the reconstituted mucus ($\phi = \tan^{-1}(G''/G') = 30^\circ$ at $\omega = 1 \text{ s}^{-1}$) showed that the viscosity and elasticity of PGM were matched similarly to physiological mucus (21). At low frequencies, PGM had strong gel-forming properties, but gelation was disrupted

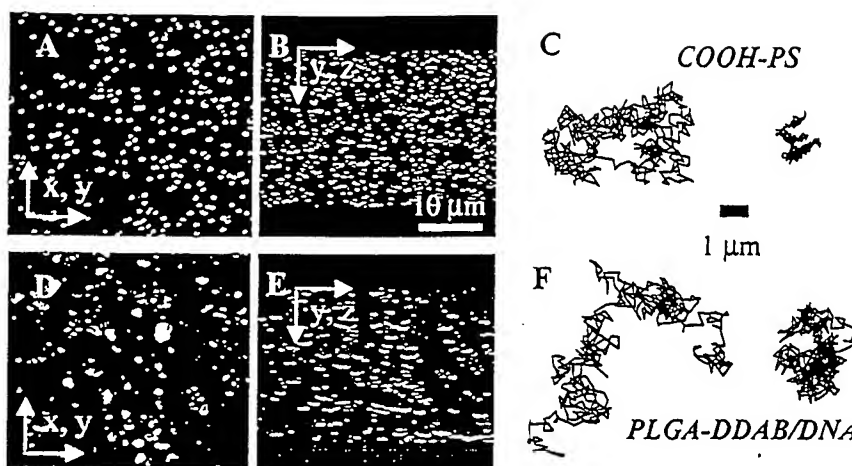


Figure 3. Reconstructed 3-D confocal images of fluorescently labeled (A, B) COOH-PS (note the uniform size and distribution) and (D, E) PLGA-DDAB/DNA nanoparticles (particle size is less uniform with aggregates). Diffusive and sub-diffusive 20-s trajectories of (C) COOH-PS and (F) PLGA-DDAB/DNA nanoparticle motion in PGM.

at shear rates corresponding to a frequency of $\omega = 2.5 \text{ s}^{-1}$. Reconstituted mucus deforms at lower shear rates than crude mucus (21). However, particle transport studies are performed on quiescent fluids in this work, and thus, mucus is not subjected to deforming shear conditions.

PLGA-DDAB/DNA and 200 nm COOH-PS Nanoparticles Embedded in PGM. Following incubation in mucus, the ζ -potential measured for carboxylated polystyrene (COOH-PS) particles (-17.5 mV at pH 6) was close to that for PLGA-DDAB/DNA nanoparticles ($-11 \pm 7 \text{ mV}$ at pH 6), even though the initial ζ -potentials of the two particle types were quite different prior to incubation with mucus (39 ± 6 for PLGA-DDAB/DNA and -5 mV for COOH-PS). This result suggests that mucus components readily adsorb to the surface of each type of particle within minutes of their addition to mucus.

Confocal microscopy was used to collect three-dimensional images of nanoparticles embedded in reconstituted PGM samples (bead solution was $\sim 3\%$ total volume) (Figure 3A, B, D, and E). COOH-PS nanoparticles showed reduced aggregation when compared to PLGA-DDAB/DNA nanoparticles, which indicated that PLGA-DDAB/DNA nanoparticles were either adhering as clumps to mucin fibers or aggregating via particle-particle interactions mediated by mucus. Adhesion to mucus may not be surprising since DDAB, which remains on the surface of PLGA-DDAB/DNA nanoparticles, is a cationic surfactant and mucin and other macromolecules found in PGM are strongly anionic (22). Note that although COOH-PS particles did not appear to aggregate heavily in mucus, they may still be adherent to mucus as individual particles (see next section).

Nanoparticle Transport Rates Measured with Multiple Particle Tracking (MPT). The mobility of COOH-PS and PLGA-DDAB/DNA nanoparticles in PGM was tracked in real time in two-dimensions. Suggesting 2-D tracking represents the 3-D mobility of particles assumes that mucus is an isotropic fluid but not necessarily homogeneous. We verified with 3-D confocal microscopy that PLGA-DDAB/DNA and COOH-PS particle distributions in mucus are independent of location within the gel in the x , y , and z directions (Figure 3).

Twenty-second trajectories of nanoparticle motion in PGM showed that PLGA-DDAB/DNA nanoparticles appeared to be considerably more mobile than COOH-PS nanoparticles (Figure 3C and F). Individual particle MSDs were used to determine the average (or "ensemble-

average") MSD, allowing the variation in particle transport rates with respect to time to be directly computed. The ensemble MSD of PLGA-DDAB/DNA nanoparticles was 10-fold higher than the ensemble MSD of 200 nm COOH-PS nanoparticles over a range of time scales (Figure 4A). Furthermore, the ensemble MSD of PLGA-DDAB/DNA nanoparticles had an almost linear dependency on time, indicating that the average transport rate in PGM was dominated by diffusive carriers. Nevertheless, particle motion is severely limited by the viscoelastic nature of PGM, as indicated by the normalized average (or "effective") diffusion coefficients, which are 50- to 500-fold lower than their theoretical diffusivities in water (Figure 4B). The normalized diffusion coefficients show that the average particle transport rate decreases slightly with respect to time (Figure 4B), which would be expected, for example, if a significant fraction of particles underwent sub-diffusive transport (for example, particles adherent to mucus fibers).

The observation that PLGA-DDAB/DNA particles moved faster on average than COOH-PS particles was somewhat counterintuitive since PLGA-DDAB/DNA nanoparticle aggregation was expected to reduce their transport rates. Therefore, to further elucidate the mode and rate of particle transport in PGM, we examined the distributions of individual particle MSDs (Figure 5). The mode of transport of each individual particle was determined by the slope of the particle MSD versus time on a log-log scale. A slope of < 1 indicated that transport was sub-diffusive, or hindered, whereas a slope of ~ 1 indicated that transport was diffusive. For time scales $< 1 \text{ s}$, COOH-PS nanoparticle MSDs were primarily sub-diffusive (Figure 5A), indicating that a majority of these particles (101 of 109, or 93%, at time scales between 0.1 and 1 s) are transiently adherent to mucus or are temporarily trapped within cages formed by mucus fibers. In contrast, considerably more PLGA-DDAB/DNA nanoparticles had diffusive MSDs at earlier time scales (Figure 5B), with only 78% (94 of 120) undergoing sub-diffusive transport at time scales between 0.1–1 s. Therefore, although a considerable fraction of PLGA-DDAB/DNA particles appear to aggregate in PGM, a significantly higher percentage of PLGA-DDAB/DNA particles (22%) undergo diffusive transport at early time scales compared to COOH-PS particles (7%).

To quantify the degree of heterogeneity in particle transport rates, the distributions of the individual MSDs of COOH-PS and PLGA-DDAB/DNA nanoparticles at

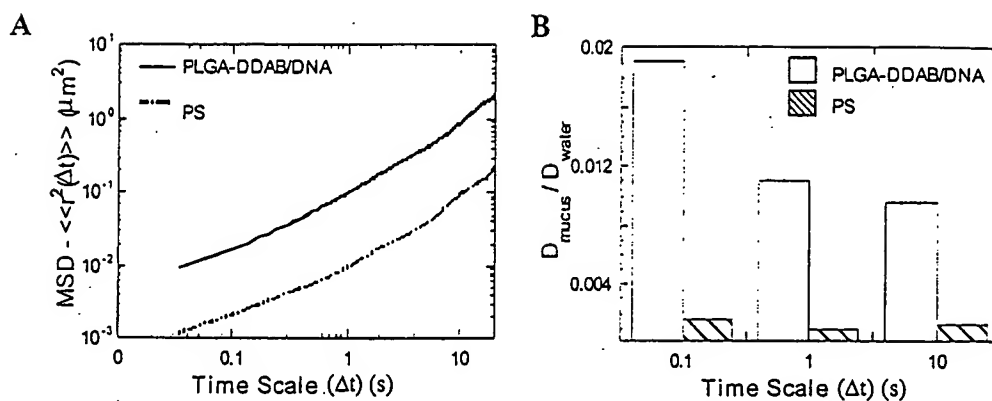


Figure 4. (A) Ensemble MSD of PLGA-DDAB/DNA and COOH-PS nanoparticles in PGM. (B) The average diffusion coefficients, normalized with the theoretical diffusivity of 200 nm particles in water, of COOH-PS and PLGA-DDAB/DNA show slight time dependence.

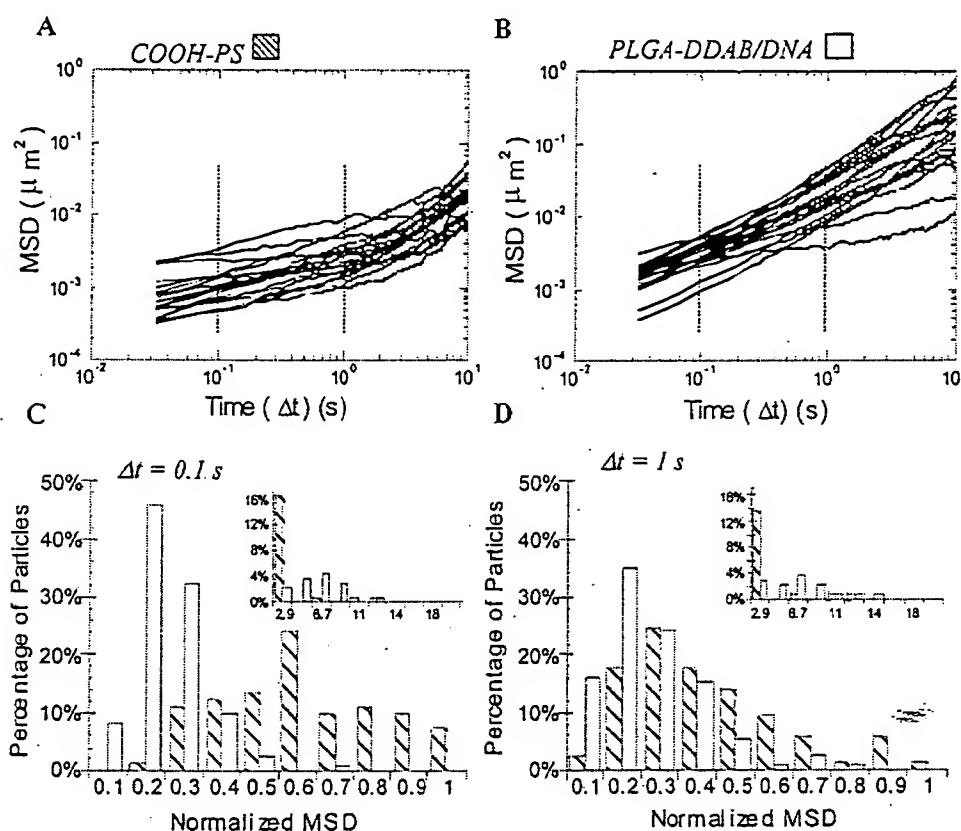


Figure 5. Twenty time-dependent particle MSDs for (A) COOH-PS and (B) PLGA-DDAB/DNA nanoparticles, randomly selected ($n = 109$ and 120 , respectively). The distribution of MSDs for COOH-PS (hatched bars) and PLGA-DDAB/DNA (open bars) particles, normalized with their respective ensemble averaged MSD, at (C) $\Delta t = 0.1$ s and (D) $\Delta t = 1$ s indicate that the majority of particles have MSDs less than the average. Note that a small percentage of faster particles largely affects the average rate of transport (see insets), especially at small time scales when many particles are moving with more sub-diffusive transport rates.

time scales of $\Delta t = 0.1$ and 1 s were normalized by their respective ensemble average MSDs (Figure 5C and D). In general, the mean MSD of each particle type was significantly smaller than the ensemble average MSD, indicating that a small percentage ($\sim 10\%$) of the particles contributed significantly to the average rate of transport. At early time scales ($\Delta t = 0.1$ s), when transport of COOH-PS nanoparticles was primarily sub-diffusive, the mean of the MSD was only 2-fold lower than the average; at larger time scales ($\Delta t = 1$ s), the mean was nearly 5-fold lower than the average. In contrast, for all time scales, PLGA-DDAB/DNA nanoparticles had mean transport rates that were 5-fold lower than the average. This result provided further evidence that a high percentage of COOH-PS nanoparticles were either transiently ad-

herent to mucus or temporarily trapped in microscopic cages in PGM over short time scales (thereby leading to a more homogeneous distribution of transport rates). Given time, some COOH-PS particles could resume diffusion by desorbing or escaping their sub-diffusive cages (leading to an increase in the heterogeneity of the particle transport rates). On the other hand, a higher number of PLGA-DDAB/DNA nanoparticles had diffusive transport rates at short time scales, leading to high heterogeneity in particle transport rates, but fewer changed their mode of transport over time, which was apparent in the similarities of the mean MSD at time scales of $\Delta t = 0.1$ and 1 s. This result suggests that, following the adhesion of a fraction of the PLGA-DDAB/DNA particles, a significant percentage of the remaining

particles were able to undergo unrestricted diffusive transport. Heterogeneities in particle transport rates may be important in assessing the efficiency of particles in traversing the mucosal barrier since gene delivery may only require a small percentage of gene carriers to reach target epithelial cells (5).

There are several possible explanations for the more rapid transport of the slightly aggregated (and thus, larger) PLGA-DDAB/DNA particles compared to COOH-PS particles. For example, Olmstead and co-workers (10) demonstrated that herpes simplex virus (HSV) particles adhere to mucin fibers found in cervical mucus, causing the fibers to collapse into coil-like structures and inducing the formation of larger pores around the condensed mucus. The rearrangement of the mucus network promoted more rapid local transport of HSV particles (10). Similarly, the observed PLGA-DDAB/DNA particle aggregates with mucus may have led to larger pores that promoted more rapid transport of PLGA-DDAB/DNA particles compared to COOH-PS particles. This hypothesis is supported indirectly by the fact that a considerably higher percentage of PLGA-DDAB/DNA nanoparticles (8.5%) exhibited a MSD greater than 5-fold of their ensemble average MSD compared to only 2.9% for COOH-PS nanoparticles, each at a time scale of 0.1 s (7.7% versus 3.9% at a time scale of 1 s for PLGA-DDAB/DNA versus COOH-PS, respectively).

A second possible explanation for the increased transport rates of PLGA-DDAB/DNA nanoparticles compared to those of the slightly smaller COOH-PS nanoparticles may be related to the difference in surface chemistries of the two particle types. PLGA-DDAB/DNA nanoparticle surfaces are coated with DNA, making them relatively hydrophilic compared to COOH-PS nanoparticles. Mucus is composed of a dense network of fibers that are relatively hydrophobic compared to the solution contained within the network pores. Therefore, it is possible that the fraction of PLGA-DDAB/DNA nanoparticles that do not interact electrostatically with negatively charged mucin glycoproteins are capable of enhanced transport in the hydrophilic mucus pores compared to COOH-PS particles, a larger fraction of which may adhere as single particles to the mucus network. This hypothesis is supported by the finding that a larger fraction of COOH-PS particles undergo sub-diffusive, or hindered, transport compared to PLGA-DDAB/DNA particles (Figure 5). The fact that each particle type appears to adsorb mucus components (as indicated by the decrease in ζ -potential for each particle upon incubation in mucus) presumably makes the particle surfaces more similar. If the entire surface is coated by mucus components, then the differences in initial surface chemistries may not be important, thus favoring the former hypothesis. Future studies aimed at quantifying the effects of particles on the pore structure of the mucus mesh and at determining the surface composition of the particles following incubation in mucus should help explain the transport phenomena observed.

Conclusions

Multiple particle tracking (MPT) was used to study transport rates of individual gene carriers in gastric mucus. Advantages of MPT include the ability to study individual particle transport and distributions of transport rates, as well as their contributions to the average or "bulk" properties, in complex biological environments (14, 23). We measured transport rates of cationic nanoparticles made from PLGA-DDAB/DNA in PGM and found that their transport rates were much higher (~10-

fold) than that of slightly smaller COOH-PS nanoparticles. It is possible for larger particles (such as the PLGA-DDAB/DNA particles) to move more rapidly through a porous media than smaller particles by, for example, altering the pore network of the mucus or by spending less time on average either physically trapped within cages formed by elastic mucus fibers or, perhaps more likely, adherent to mucus fibers. Regardless, rapid transport through mucus and the ability to transfect cells make PLGA-DDAB/DNA particles interesting for further in vitro and in vivo testing as gene delivery agents.

Acknowledgment

The authors acknowledge Tom Kole and Yiider Tseng for technical assistance with multiple particle tracking and Junghae Suh, Stephanie Kim, and Dave McGovern for technical assistance. The authors acknowledge financial support from the National Science Foundation (CTS0210718) and the Whitaker Foundation (RG-99-0046) and fellowship funding from the National Science Foundation, the Ford Foundation, and ARCS.

References and Notes

- (1) Singh, M.; Briones, M.; Ott, G.; O'Hagan, D. Cationic microparticles: A potent delivery system for DNA vaccines. *Proc. Natl. Acad. Sci. U.S.A.* 2000, 97, 811-816.
- (2) Singh, M.; Ott, G.; Kazzaz, J.; Ugozzoli, M.; Briones, M. et al. Cationic microparticles are an effective delivery system for immune stimulatory CpG DNA. *Pharm. Res.* 2001, 18, 1476-1479.
- (3) Singh, M.; Vajdy, M.; Gardner, J.; Briones, M.; O'Hagan, D. Mucosal immunization with HIV-1 gag DNA on cationic microparticles prolongs gene expression and enhances local and systemic immunity. *Vaccine* 2001, 20, 594-602.
- (4) McGehee, J. R.; Lamm, M. E.; Strober, W. Mucosal immune responsees. In *Mucosal Immunology*, 2nd ed.; Academic Press: San Diego, 1999; pp 485-506.
- (5) Hanes, J.; Dawson, M.; Har-el, Y.; Suh, J.; Fiegel, J. Gene therapy in the lung. In *Pharmaceutical Inhalation Aerosol Technology*, 2nd ed.; Marcel Dekker Inc.: New York, 2003; pp 489-539.
- (6) Kumar, M.; Behera, A. K.; Lockey, R. F.; Zhang, J.; Bhullar, G. et al. Intranasal gene transfer by chitosan-DNA nanoparticles protects BALB/c mice against acute respiratory syncytial virus infection. *Hum. Gene Ther.* 2002, 13, 1415-1425.
- (7) Khanvilkar, K.; Donovan, M. D.; Flanagan, D. R. Drug transfer through mucus. *Adv. Drug Deliv. Rev.* 2001, 48, 173-193.
- (8) Saltzman, W. M.; Radomsky, M. L.; Whaley, K. J.; Cone, R. A. Antibody diffusion in human cervical mucus. *Biophys. J.* 1994, 66, 508-515.
- (9) Sanders, N. N.; De Smedt, S. C.; Van Rompaey, E.; Simoens, P.; De Baets, F. et al. Cystic fibrosis sputum: a barrier to the transport of nanospheres. *Am. J. Respir. Crit. Care Med.* 2000, 162, 1905-1911.
- (10) Olmsted, S. S.; Padgett, J. L.; Yudin, A. I.; Whaley, K. J.; Moench, T. R. et al. Diffusion of macromolecules and virus-like particles in human cervical mucus. *Biophys. J.* 2001, 81, 1930-1937.
- (11) Cone, R. A. Mucus. In *Mucosal Immunology*, 2nd ed.; Academic Press: San Diego, CA, 1999; pp 43-64.
- (12) Miller, J. Assay of B-galactosidase. In *Experiments in Molecular Genetics*; Miller, J., Ed.; Cold Spring Harbor Laboratory: Cold Spring Harbor, 1972; pp 352-355.
- (13) Tseng, Y.; Fedorov, E.; McCaffery, J. M.; Almo, S. C.; Wirtz, D. Micromechanics and ultrastructure of actin filament networks cross-linked by human fascin: a comparison with alpha-actinin. *J. Mol. Biol.* 2001, 310, 351-366.
- (14) Dawson, M.; Wirtz, D.; Hanes, J. Enhanced viscoelasticity of human cystic fibrotic sputum correlates with increasing microheterogeneity in particle transport. *J. Biol. Chem.* 2003, 278, 50393-50401.

- 583 (15) Apgar, J.; Tseng, Y.; Fedorov, E.; Herwig, M. B.; Almo, S.
584 C. et al. Multiple-particle tracking measurements of hetero-
585 geneities in solutions of actin filaments and actin bundles.
586 *Biophys. J.* 2000, 79, 1095–1106.
587 (16) Tseng, Y.; Wirtz, D. Mechanics and multiple-particle
588 tracking microheterogeneity of alpha-actinin-cross-linked ac-
589 tin filament networks. *Biophys. J.* 2001, 81, 1643–1656.
590 (17) Denis-Mize, K. S.; Dupuis, M.; MacKichan, M. L.; Singh,
591 M.; Doe, B. et al. Plasmid DNA adsorbed onto cationic
592 microparticles mediates target gene expression and antigen
593 presentation by dendritic cells. *Gene Ther.* 2000, 7, 2105–
594 2112.
595 (18) Ferrari, S.; Kitson, C.; Farley, R.; Steel, R.; Marriott, C. et
596 al. Mucus altering agents as adjuncts for nonviral gene trans-
597 fer to airway epithelium. *Gene Ther.* 2001, 8, 1380–1386.
598 (19) Yonemitsu, Y.; Kitson, C.; Ferrari, S.; Farley, R.; Griesen-
599 bach, U. et al. Efficient gene transfer to airway epithelium
using recombinant Sendai virus. *Nat. Biotechnol.* 2000, 18, 600
970–973. 601
(20) Quraishi, M. S.; Jones, N. S.; Mason, J. The rheology of 602
nasal mucus: a review. *Clin. Otolaryngol.* 1998, 23, 403– 603
413. 604
(21) Rogunova, M. A.; Blackwell, J.; Jamieson, A. M.; Pasumar- 605
thy, M.; Gerken, T. A. Effects of lipid on the structure and 606
rheology of gels formed by canine submaxillary mucin. 607
Biorheology 1997, 34, 295–308. 608
(22) Norris, D., Sinko, P. *J. Appl. Polym. Sci.* 63, 1481–1492. 609
(23) Suh, J.; Wirtz, D.; Hanes, J. Efficient active transport of 610
gene nanocarriers to the cell nucleus. *Proc. Natl. Acad. Sci.* 611
U.S.A. 2003, 100, 3878–3882. 612
- Accepted for publication January 7, 2004. 613
BP0342553 614

TRANSPORT OF POLYMERIC NANOPARTICLE GENE CARRIERS IN GASTRIC MUCUS

Michelle Dawson¹, Eric Krauland², Denis Wirtz^{1,3}, Justin Hanes^{1,2}

Departments of ¹Chemical and Biomolecular Engineering, ²Biomedical Engineering, and

³Materials Science and Engineering, The Johns Hopkins University, Baltimore, MD.

Correspondence:

Justin Hanes, Assistant Professor

Department of Chemical and Biomolecular Engineering

Johns Hopkins University, 3400 N. Charles Street, Baltimore, MD, 21218

Phone: (410) 516-3484; Fax: (410) 516-5510; email address: hanes@jhu.edu.

Abbreviations used in this paper. MPT, multiple-particle tracking; MSD, mean squared displacement; PLGA, poly(D,L-lactic-co-glycolic) acid; DDAB, dimethyldioctadecyl ammonium bromide; COOH-PS, carboxylated polystyrene.

Keywords:

Gene delivery, nanoparticle transport, mucus, mucosal barrier, mucosal vaccines, and cationic nanoparticles.

RECEIVED JAN 16 2004

INTRODUCTION

Cationic polymeric microparticles have previously been shown to efficiently condense DNA, leading to non-cytotoxic gene carriers capable of stable gene expression in small animal models following intramuscular injection (1-3). In these studies, the effective dosage of DNA was reduced from 1—2 mg to 1—10 µg, a result attributed to the reduced degradation of DNA (since encapsulation leads to DNA degradation) and the enhanced amount of DNA immediately available to induce an immune response.

Mucosal immunization is of considerable interest since gastrointestinal, nasal, respiratory, and vaginal mucosal tissues all drain to lymph nodes, leading to both local and distal immune responses (4). Thus, immunization of one mucosal surface can lead to long-term protective immune responses on all other mucosal surfaces. However, the effectiveness of cationic nanoparticles to deliver DNA to mucosal sites relies on the ability of these particles to cross mucosal barriers (5,6).

The primary component of mucus is high molecular weight mucin glycoproteins, which form numerous covalent and non-covalent bonds with other mucin molecules and various constituents, including DNA, alginate, and hyaluronan (5). Reconstituted mucus formulated from pig gastric, human cervical and tracheobronchial mucins display similar mucus structures, with large rod or fiber-like aggregates of 5 nm in diameter and 100-5000 nm in length (7). The condensed and complex microstructure of the mucus network gives rise to a highly viscoelastic gel, which significantly impedes the transport rates of large macromolecules and nanoparticles (8-10). Immobilized nanoparticles are subject to bacterial and enzymatic degradation and may also be cleared from the body by normal mucus clearance mechanisms. Although clearance rates are anatomically determined, mucus turnover rates in the GI tract are estimated as between 24-48

MATERIALS AND METHODS

Materials

Poly (D,L-lactic-co-glycolic) (PLGA) (Medisorb High I.V. 54:46) was obtained from Alkermes (Cincinnati, OH), and 1,2-diacyl-palmitoyl-glycerol-3-phosphocholine (DPPC) was purchased from Avanti Polar Lipids (Alabaster, AL). Dimethyl dioctadecyl ammonium bromide (DDAB), bovine serum albumin (BSA), pig gastric mucin (PGM), and deoxyribonucleic acid (DNA) (sodium salt, from salmon testes) were purchased from Sigma (St. Louis, MO) and used without further purification. 2,2,2-Trifluoroethanol (TFE) was purchased from Fluka (Milwaukee, WI). Plasmid DNA was extracted from *Escherichia coli* culture (strain DH5a, plasmid p43-clz1, kindly donated by Dr. Kam Leong, Johns Hopkins University) grown in freshly prepared Luria Bertani (LB) broth supplemented with 100mg/mL ampicillin (Kodak Chemicals, Rochester, NY) using a Endo-free Qiagen Megaprep (Valencia, CA), and subsequently resuspended in sterile, deionized water. The plasmid p43-clz1 contains the β -galactosidase gene under the human early-intermediate cytomegalovirus (CMV) promoter and also contains a gene for ampicillin resistance. All other solutions and reagents were of analytical grade and used without further purification.

Formulation of Cationic PLGA Nanoparticles

Particles were prepared by a solvent extraction/precipitation method. PLGA (3 mg/ml) and DDAB (10 mg/ml) were dissolved in TFE separately. Subsequently, 3 ml PLGA solution (9 mg PLGA) and 200 μ l of DDAB solution (2 mg DDAB) were combined and added dropwise to 8 mL of filtered distilled water stirring on a magnetic plate. Next, 100 μ L of 1 mg/ml salmon testes DNA in distilled water was added to the water/TFE mixture and stirred for 3 hours on a

process. Twenty μL of sample was run on an ethidium bromide stained 1.0% agarose gel (70 V for 60 min) in TAE buffer (Tris-Acetate-EDTA).

Nanoparticle and Naked DNA Transfections with Lac-Z Reporter Gene

Cos-7 cells were obtained from American Type Culture Collection (ATCC, Rockville, MD) and maintained in Dulbecco's Modified Eagle's Medium (DMEM) (Gibco, BRL) containing 10% fetal bovine serum (Gibco, BRL, Invitrogen Co., Carlsbad, CA). Cells seeded at a density of 1.8×10^6 cells/cm² on 35-mm 6-well plates were transfected at 50-60% confluency with PLGA-DDAB/DNA nanoparticles or plasmid DNA alone (the concentration in all cases was maintained to yield 2.5 μg DNA per well, or 0.26 μg DNA/cm²). Cells were harvested 48 hours after transfection. β -galactosidase activity and total protein content were assayed using the standard β -galactosidase spectrophotometric assay (12) and the manufacturer's given micro-well protocol for the BCA assay (Pierce Chemical Co., Rockford, IL), respectively. Reported values of β -galactosidase expression were normalized to the total protein content per sample well ($n = 3$).

The toxicity of PLGA-DDAB/DNA nanoparticles to Cos-7 cells was assayed using a propidium iodide nucleic acid stain (Molecular Probes; Eugene, OR). Cos-7 cells seeded at 1×10^6 cells/cm² were allowed to reach 60% confluency and then incubated with PLGA-DDAB/DNA nanoparticles, naked DNA, or PolyFect/DNA particles and harvested after 48 hours. The PLGA-DDAB/DNA particle volume was adjusted to give final DNA amounts of 1.0, 2.5, and 5.0 μg per well, while naked DNA and PolyFect/DNA concentrations were adjusted to result in a final DNA content of 2.5 μg per well. Harvested cells were resuspended in 500 $\mu\text{g}/\text{ml}$ propidium iodide solution, which intercalates with DNA released from necrotic cells. The

with condensed salmon testes DNA (35 mV, 196 ± 29 nm diameter) in reconstituted PGM were recorded using a silicon-intensified target camera (VE-1000, Dage-MTI, Michigan, IN) mounted on an inverted epifluorescence microscope equipped with 100X oil-immersion objective (numerical aperture 1.3). The trajectories of $n=109$ COOH-PS and $n=120$ PLGA-DDAB/DNA particles were tracked in PGM samples contained within a microscope chamber maintained at 37° C.

The centroid of each particle was tracked with 5 nm spatial resolution, determined by tracking the apparent displacements of microspheres immobilized on a glass microslide with a strong adhesive (15). Nanoparticle motion was tracked in 2-D by following the motion of nanoparticles in the plane of focus. For 2-D displacements to accurately represent 3-D motion, the fluid must be isotropic, but need not be homogeneous (14). Images of the microspheres were captured with a custom routine incorporated in the Metamorph software (Universal Imaging Corp.) at a frequency of 30 Hz for 20 s, which gives a temporal resolution of 33 ms. The coordinates of nanoparticle centroids were transformed into families of time-averaged mean squared displacements (MSD), $\langle \Delta r^2(\tau) \rangle = \langle [x(t+\tau) - x(t)]^2 + [y(t+\tau) - y(t)]^2 \rangle$ (τ = time scale or time lag), from which distributions of MSDs and time-dependent particle diffusion coefficients ($D(\tau) = \langle \Delta r^2(\tau) \rangle / 4\tau$) were calculated as previously demonstrated (16). Diffusion coefficients were normalized with the theoretical diffusion coefficient of 200 nm particles in water as determined by the classical Stokes-Einstein equation.

study) resulting in background levels of cell toxicity (7.2 ± 0.6 % dead cells, not significantly different than naked DNA controls). Singh and coworkers reported that PLGA-DDAB/DNA microparticles caused no acute toxicity with particle doses resulting in the equivalent of 1 mg of DNA per animal (guinea pig) (1).

Incubation of PLGA-DDAB/DNA nanoparticles in mucus for < 30 minutes changed the average particle surface charge from 39 ± 6 mV to -11 ± 7 mV, and the average particle size increased from 196 ± 29 nm to 249 ± 21 nm. The change in size and surface charge of PLGA-DDAB/DNA particles indicated that mucus constituents adsorbed on particle surfaces, leading to a significant increase in particle diameter.

Rheological Characterization of PGM

The highly viscoelastic properties and gel formation of mucus (phase angle $< 45^\circ$) arise primarily from the high molecular weights and expanded conformations of mucin glycoproteins in aqueous solution. The ability of mucus to undergo gelation is also strongly affected by the concentrations of lipids and macromolecules, which non-covalently interact with mucins promoting the formation of larger mucin fibers that overlap to form dense mucus networks (20,21). Physiologically, the high viscoelasticity of mucus gels is maintained to provide a barrier to microbial and particle transport; high elasticity also allows mucus to be engaged by ciliated cells or moved by pulsatory forces as it is cleared from the body (20). The viscous and elastic properties are properly matched *in vivo* to achieve appropriate mucus clearance rates (5,20).

The frequency-dependent elastic and viscous moduli were used to characterize the viscoelastic nature of reconstituted pig gastric mucus (PGM) used in this study (Fig. 2). The phase angle of the reconstituted mucus ($\phi = \tan^{-1}(G''/G') = 30^\circ$ at $\omega = 1 \text{ s}^{-1}$) showed that the

Nanoparticle Transport Rates Measured with Multiple Particle Tracking (MPT)

The mobility of COOH-PS and PLGA-DDAB/DNA nanoparticles in PGM was tracked in real time in two-dimensions. Suggesting 2-D tracking represents the 3-D mobility of particles assumes that mucus is an isotropic fluid, but not necessarily homogeneous. We verified with 3-D confocal microscopy that PLGA-DDAB/DNA and COOH-PS particle distributions in mucus are independent of location within the gel in the x, y and z directions (Fig. 3).

Twenty-second trajectories of nanoparticle motion in PGM showed that PLGA-DDAB/DNA nanoparticles appeared to be considerably more mobile than COOH-PS nanoparticles (Fig. 3C and F). Individual particle MSDs were used to determine the average (or “ensemble-average”) MSD, allowing the variation in particle transport rates with respect to time to be directly computed. The ensemble MSD of PLGA-DDAB/DNA nanoparticles was 10-fold higher than the ensemble MSD of 200 nm COOH-PS nanoparticles over a range of time scales (Fig. 4A). Furthermore, the ensemble MSD of PLGA-DDAB/DNA nanoparticles had an almost linear dependency on time, indicating that the average transport rate in PGM was dominated by diffusive carriers. Nevertheless, particle motion is severely limited by the viscoelastic nature of PGM, as indicated by the normalized average (or “effective”) diffusion coefficients, which are 50-500-fold lower than their theoretical diffusivities in water (Fig. 4B). The normalized diffusion coefficients show that the average particle transport rate decreases slightly with respect to time (Fig. 4B), which would be expected, for example, if a significant fraction of particles underwent sub-diffusive transport (for example, particles adherent to mucus fibers).

The observation that PLGA-DDAB/DNA particles moved faster on average than COOH-PS particles was somewhat counterintuitive since PLGA-DDAB/DNA nanoparticle aggregation

of COOH-PS nanoparticles were either transiently adherent to mucus or temporarily trapped in microscopic cages in PGM over short time scales (thereby leading to a more homogeneous distribution of transport rates). Given time, some COOH-PS particles could resume diffusion by desorbing or escaping their sub-diffusive cages (leading to an increase in the heterogeneity of the particle transport rates). On the other hand, a higher number of PLGA-DDAB/DNA nanoparticles had diffusive transport rates at short time scales, leading to high heterogeneity in particle transport rates, but fewer changed their mode of transport over time, which was apparent in the similarities of the mean MSD at time scales of $\Delta t = 0.1$ s and 1 s. This result suggests that, following the adhesion of a fraction of the PLGA-DDAB/DNA particles, a significant percentage of the remaining particles were able to undergo unrestricted diffusive transport. Heterogeneities in particle transport rates may be important in assessing the efficiency of particles in traversing the mucosal barrier since gene delivery may only require a small percentage of gene carriers to reach target epithelial cells (5).

There are several possible explanations for the more rapid transport of the slightly aggregated (and thus, larger) PLGA-DDAB/DNA particles compared to COOH-PS particles. For example, Olmstead and coworkers (10) demonstrated that herpes simplex virus (HSV) particles adhere to mucin fibers found in cervical mucus, causing the fibers to collapse into coil-like structures and inducing the formation of larger pores around the condensed mucus. The rearrangement of the mucus network promoted more rapid local transport of HSV particles (10). Similarly, the observed PLGA-DDAB/DNA particle aggregates with mucus may have led to larger pores that promoted more rapid transport of PLGA-DDAB/DNA particles compared to COOH-PS particles. This hypothesis is supported indirectly by the fact that a considerably higher percentage of PLGA-DDAB/DNA nanoparticles (8.5%) exhibited an MSD greater than 5-

CONCLUSIONS

Multiple particle tracking (MPT) was used to study transport rates of individual gene carriers in gastric mucus. Advantages of MPT include the ability to study individual particle transport and distributions of transport rates, as well as their contributions to the average or "bulk" properties, in complex biological environments (14,23). We measured transport rates of cationic nanoparticles made from PLGA-DDAB/DNA in PGM and found that their transport rates were much higher (~10-fold) than that of slightly smaller COOH-PS nanoparticles. It is possible for larger particles (such as the PLGA-DDAB/DNA particles) to move more rapidly through a porous media than smaller particles by, for example, altering the pore network of the mucus or by spending less time on average either physically trapped within cages formed by elastic mucus fibers or, perhaps more likely, adherent to mucus fibers. Regardless, rapid transport through mucus and the ability to transfect cells make PLGA-DDAB/DNA particles interesting for further *in vitro* and *in vivo* testing as gene delivery agents.

ACKNOWLEDGEMENTS

Authors acknowledge Tom Kole and Yiider Tseng for technical assistance with multiple particle tracking and Junghae Suh, Stephanie Kim, and Dave McGovern for technical assistance. The authors acknowledge financial support from the National Science Foundation (CTS0210718), the Whitaker Foundation (RG-99-0046), and fellowship funding from the National Science Foundation, the Ford Foundation, and ARCS.

- (18) Ferrari, S.; Kitson, C.; Farley, R.; Steel, R.; Marriott, C. et al. Mucus altering agents as adjuncts for nonviral gene transfer to airway epithelium. *Gene Ther* 2001, 8, 1380-1386.
- (19) Yonemitsu, Y.; Kitson, C.; Ferrari, S.; Farley, R.; Griesenbach, U. et al. Efficient gene transfer to airway epithelium using recombinant Sendai virus. *Nat Biotechnol* 2000, 18, 970-973.
- (20) Quraishi, M. S.; Jones, N. S.; Mason, J. The rheology of nasal mucus: a review. *Clin Otolaryngol* 1998, 23, 403-413.
- (21) Rogunova, M. A.; Blackwell, J.; Jamieson, A. M.; Pasumar-Thy, M.; Gerken, T. A. Effects of lipid on the structure and rheology of gels formed by canine submaxillary mucin. *Biorheology* 1997, 34, 295-308.
- (22) Norris, D., Sinko, P *J Appl Polym Sci*, 63, 1481-1492.
- (23) Suh, J.; Wirtz, D.; Hanes, J. Efficient active transport of gene nanocarriers to the cell nucleus. *Proc Natl Acad Sci U S A* 2003, 100, 3878-3882.

Figure 1.

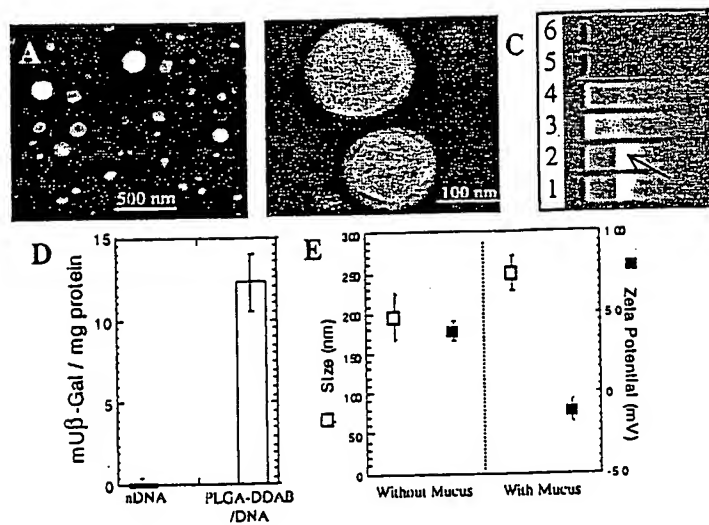


Figure 3.

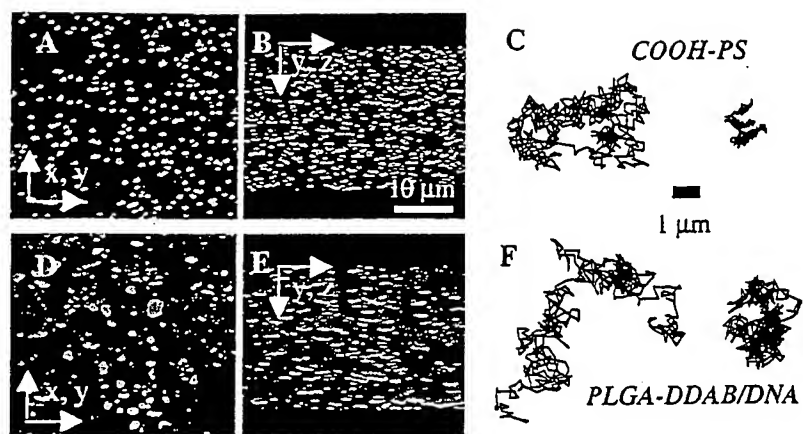


Figure 5.

